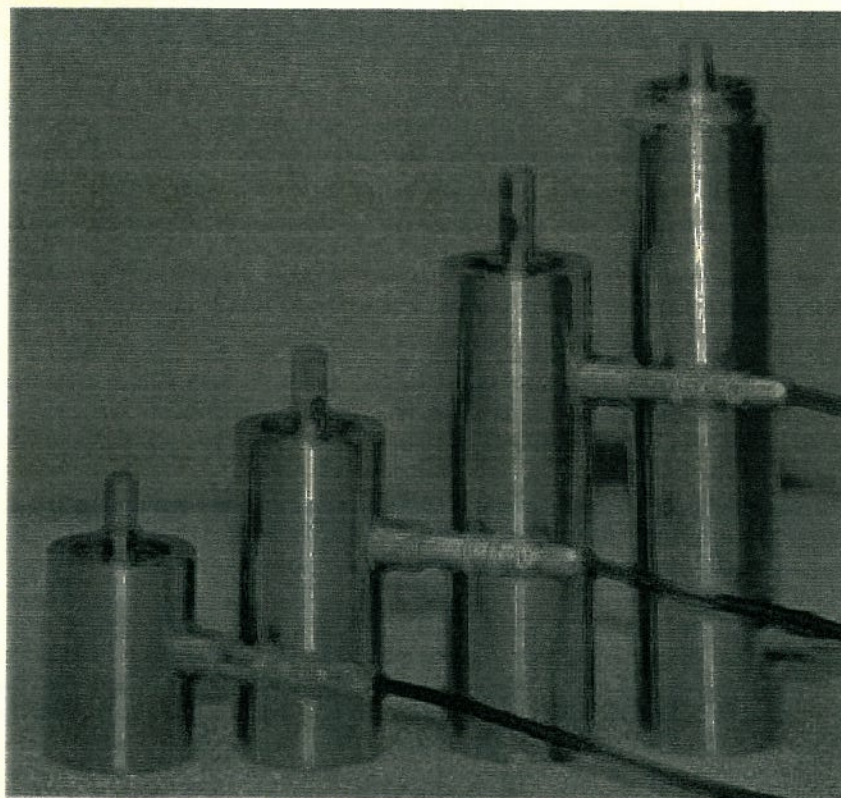




# Energy-Based Comparison of Solid-State Actuators

Victor Giurgiutiu  
Radu Pomirleanu  
Craig A. Rogers



Report # USC-ME-LAMSS-2000-102, March 1, 2000.

Laboratory for Adaptive Materials and Smart Structures  
University of South Carolina  
Columbia, SC 29208

## ENERGY-BASED COMPARISON OF SOLID-STATE ACTUATORS

Victor Giurgiutiu, Radu Pomirleanu and Craig A. Rogers

LABORATORY FOR ADAPTIVE MATERIALS AND SMART STRUCTURES,

UNIVERSITY OF SOUTH CAROLINA

COLUMBIA, SC 29028, USA

PHONE 803 777-8018, FAX 803 777-0106, E-MAIL [victorg@sc.edu](mailto:victorg@sc.edu)

### ABSTRACT

A study of published literature and information from piezoelectric, electrostrictive, and magnetostrictive actuator vendors has been undertaken to establish the mechanical and electrical operating characteristics of the actuators under quasi-static conditions, and to compare them using output energy density criteria. Output energy values of up to 0.720 J can be achieved with off-the-shelf actuators. Energy density per unit volume of active material was found in the range 2.3-7.5 J/dm<sup>3</sup>. Energy density per unit mass of active material was found in the range 0.31-0.96 J/kg. Energy transformation efficiency between input electric energy and output mechanical energy was found to be: 11.7-35% for adhesively-bonded PZT and PMN stacks. The overall performance of induced-strain actuators based on output energy density criteria was found to vary widely from vendor to vendor, and even from one model to another within the same vendor catalogue list. These variations are attributed to progress being made currently in both the active material technology and in the detailed mechanical construction of induced-strain actuators based on these materials.

### INTRODUCTION

The use of solid-state induced-strain actuators has experienced a great expansion in recent years. Initially developed for high-frequency, low-displacement acoustic applications, these revolutionary concepts are currently expanding in their field of application in many other areas of mechanical and aerospace design. Compact and reliable, induced-strain actuators directly transform the input electrical energy into output mechanical energy. One application area in which solid-state induced-strain devices have a very promising perspective is that of linear actuation. At the moment, the linear actuation market is dominated by hydraulic and pneumatic cylinders, and by electromagnetic solenoids and shakers. Hydraulic and pneumatic cylinders offer reliable performance, with high force and large displacement capabilities. When equipped with servovalves, the hydraulic cylinders can deliver variable stroke output over a relatively large frequency range. Servovalve-controlled hydraulic devices are the actuator of choice for most aerospace, automotive, and robotic applications. However, a major drawback in the use of conventional hydraulic actuators is the need for a separate hydraulic power unit equipped with large electric motors and hydraulic

pumps that send the high-pressure hydraulic fluid to the actuators through hydraulic lines. These features can be a major drawback in certain applications; for example, in the actuation of a servo-tab placed at the tip of a rotating blade, the high-g environment, and the fact that the blade rotates, prohibit the use of conventional hydraulics. In such situations, an electro-mechanical actuation that directly converts electrical energy into mechanical energy is preferred. Conventional electro-mechanical actuator devices, that are based on electric motors, either deliver only rotary motion or require gearboxes and eccentric mechanisms to achieve linear motion. This route is cumbersome and leads to additional weight being added to that of the device, thus reducing its design effectiveness. Linear-action electromechanical devices, such as solenoids and electrodynamic shakers, exist, but are known for their typical low-force performance. The use of solenoids or electrodynamic shakers to perform the actuator duty-cycle of hydraulic cylinders is not presently conceivable.

Solid-state induced-strain actuators offer a viable alternative. Though their output displacement is



## New materials

The inherent small strain capabilities and the hysteresis behavior of the above-presented ceramic materials prompted more research.

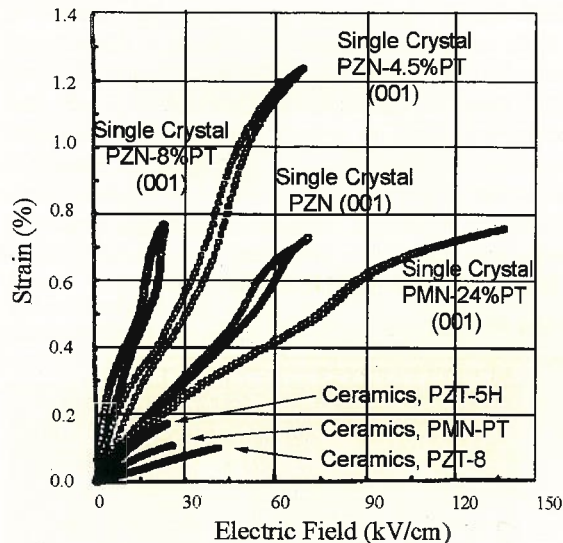


Figure 1 Strain vs. E-field behavior for <001> oriented rhombohedral crystals of PZN-PT and PMN-PT and various piezoceramics (Park and Shrout, 1997).

One direction is represented by single crystal materials. Park and Shrout (1997) reported strain levels of up to 1.5% for single crystals of relaxor perovskite  $\text{Pb}(\text{Zn}_{1/3}\text{Nb}_{2/3})\text{O}_3 - \text{PbTiO}_3$ , maintaining in the same time a reduced hysteresis, as shown in Figure 1. Single crystal material characteristics as reported by TRS are given in Table 2.

The design of the actuators that use the PZN-PT material must take into account the strong dependence of the piezoelectric properties on the crystal orientation (see Figure 2). Although this fact can be regarded as an optimization criterion in the design of actuators, it implies a reduced versatility when compared with piezoceramic materials.

Table 2 Single crystal properties (TRS Ceramics Inc.)

$K_3^T$	5000
$T_{\max}$ ( $^{\circ}\text{C}$ )	152
$d_{33}$ (pC/N)	2000
$d_{31}$ (pC/N)	-950
$s_{33}^E$ ( $10^{-12}$ m <sup>2</sup> /N)	120
$s_{31}^E$ ( $10^{-12}$ m <sup>2</sup> /N)	65
$k_{33}$	0.91
$k_{31}$	0.50
Density (g/cm <sup>3</sup> )	8.2

With this PZN-PT new material, TRS Ceramics Inc. reports building a prototype actuator with a maximum strain around 0.3%. Although no commercial version of this actuator is available at the moment, the PZN-PT material holds potential that is likely to be used in the future.

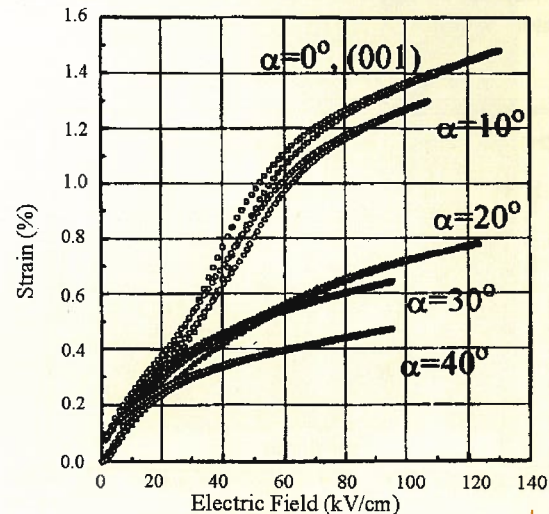


Figure 2 Strain vs. electric field (unipolar) for PZN-PT crystals oriented along (001)+ $\alpha$ , where  $\alpha$  is the degree of deviation from (001) toward (111) (Park and Shrout, 1995)

Another interesting research direction is to drive the shape memory alloys with other fields than temperature. The advantage consists mainly in the increase of the actuation speed.

Furuya *et al.* (1998) proposed a rapidly solidified ferromagnetic shape memory Fe-29.6at%Pd alloy that shows magnetostriction of up to 1800 microstrain at an applied magnetic field of  $8 \times 10^5$  A/m.

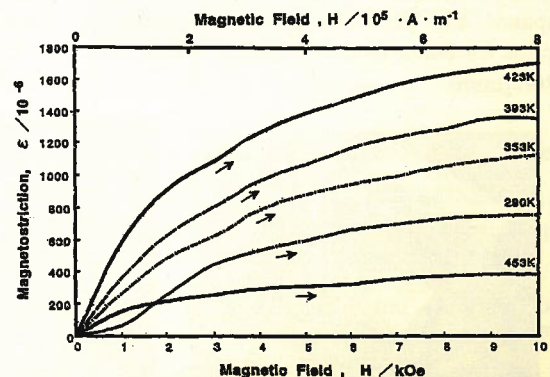


Figure 3 Changes of magnetostriction vs. magnetic field curves with increasing temperature in melt-spun Fe-29.6at%Pd alloy thin plate (roll speed 28.3 m/s, 900 $^{\circ}\text{C}$ , 1h annealed, phase transformation temperature 163 $^{\circ}\text{C}$ ) (Furuya *et al.*, 1998)



relatively small, they can produce remarkably high force. Through the use of well-architected displacement amplification, induced-strain actuators can achieve dynamic output strokes similar to those of conventional hydraulic actuators. Additionally, unlike conventional hydraulic actuators, solid-state induced-strain actuators do not require separate hydraulic power units and long hydraulic lines, and use the much more efficient route of direct electric supply to the actuator site.

The development of solid-state induced-strain actuators has entered the production stage, and actual actuation devices based on these concepts are likely to reach the applications market in the next few years. An increasing number of vendors are producing and marketing solid-state actuation devices based on induced-strain principles. However, the performance of the basic induced-strain actuation materials used in these devices, and the design solutions used in their construction, are found to vary from vendor to vendor. This variability aspect presents a difficulty for the application engineer who simply wants to utilize the solid-state induced-strain actuators as prime movers in their design, and does not intend to detail the intricacies of active materials technology.

Recognizing this need, the present paper sets out to perform a comparison of commercially-available induced-strain actuators based on a common criterion: the amount of energy that they can deliver, and the density of this energy per unit volume, unit mass, and unit cost. Additionally, this paper also compares the efficiency with which various induced-strain actuators convert the input electrical energy into output mechanical energy for use in the application.

The comparison is done using vendor-supplied information collected in an extensive survey performed over approximately a one-year period.

## BASIC ASPECTS OF INDUCED-STRAIN ACTUATORS

### Electroactive and Magnetoactive Materials

Active materials exhibit induced-strain actuation (ISA)<sup>1</sup> under the action of an electric or magnetic field. They are primarily of three types:

- PZT - Lead Zirconate Titanate - A ferroelectric ceramic material with piezoelectric properties and reciprocal behavior that converts electrical energy into mechanical energy and vice-versa. A variety

of PZT formulations have been developed to suit a wide range of signal transmission and reception qualities. PZT-5 is one of the most widely used formulation for actuator applications. It is convenient to classify the ceramic materials according to their coercive field in the field-induced strain. The material with a coercive field larger than 10 kV/cm is called a "hard" piezoelectric, which shows a wide linear drive region, but relatively small strain magnitude. The material with a coercive field between 1-10kV/cm is called a "soft" piezoelectric, which shows a large field induced strain, but relatively large hysteresis. These differences are apparent in Table 1, when the values for the piezoelectric coefficients ( $d_{33}$ ,  $d_{31}$ ,  $d_{15}$ ) and mechanical loss ( $Q_m$ ) are considered.

- PMN - Lead Magnesium Niobate - An electrostrictive ceramic material with piezoelectric properties and reciprocal behavior that converts electrical energy into mechanical energy and vice-versa. Numerous PMN formulations have been developed to suit a wide range of signal transmission and reception qualities.
- TERFENOL - TER (Terbium) FE (Iron) NOL (Naval Ordnance Laboratory) - A magnetostrictive alloy consisting primarily of Terbium, Dysprosium, and Iron. This magnetostrictive material does not exhibit reciprocal behavior since it only converts electromagnetic energy into mechanical energy. Various TERFENOL formulations have been developed. A commonly used formulation is TERFENOL-D.

Table 1 Mechanic and dielectric properties for piezoelectric and electrostrictive materials

Property	Soft PZT Navy TypeVI	Hard PZT Navy TypeIII	PMN EC- 98
$\rho$ (kg/m <sup>3</sup> )	7600	7600	7850
$k_{31}$	0.36	0.31	0.35
$k_{33}$	0.71	0.61	0.72
$k_{15}$	0.67	0.54	0.67
$d_{31}$ ( $\times 10^{-12}$ m/V)	-270	-100	-312
$d_{33}$ ( $\times 10^{-12}$ m/V)	550	220	730
$d_{15}$ ( $\times 10^{-12}$ m/V)	720	320	825
$g_{31}$ ( $\times 10^{-3}$ Vm/N)	-9.0	-11.3	-6.4
$g_{33}$ ( $\times 10^{-3}$ Vm/N)	18.3	24.9	15.6
$g_{15}$ ( $\times 10^{-3}$ Vm/N)	23.9	36.2	17
$s_{11}^E$ ( $\times 10^{-12}$ m <sup>2</sup> /N)	15.9	10.6	16.3
Poisson ratio	0.31	0.31	0.34
$s_{33}^E$ ( $\times 10^{-12}$ m <sup>2</sup> /N)	20.2	13.2	21.1
Curie Temp. (°C)	200	350	170
Mechanical $Q_m$	75	900	70

<sup>1</sup> The acronym ISA is used to signify either an induced-strain actuator, or the induced-strain actuation principle



The material also holds its dependency on temperature (see Figure 3). Furuya *et al.* (1998), also investigated the dynamic response under the alternative magnetic field and have confirmed that the magnitude of striction of the Fe-Pd foil is at least ten times greater than that of the conventional Fe-based magnetostrictive materials at 10 Hz. The response signal can be confirmed up to 100 Hz, which is 20 times faster than that of thermal SMA actuator material.

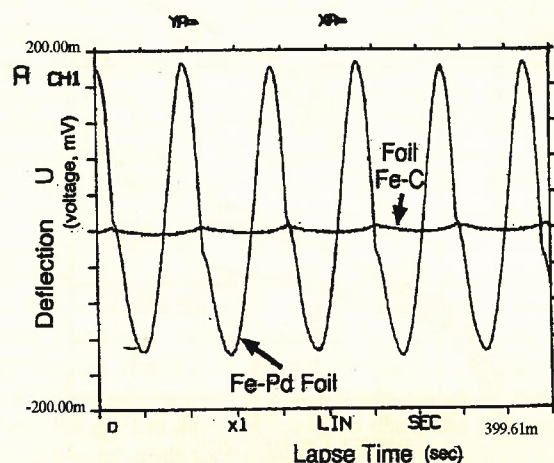


Figure 4 The cyclic strain response of rapidly solidified Fe-Pd foil and Fe-C foil as a reference at  $H=0.3$  kOe at 10Hz in solenoid-type coil (Furuya *et al.*, 1998).

#### Construction of a PZT or PMN Stack Actuator

An electroactive solid-state actuator consists of a stack of many layers of electroactive material (PZT or PMN) alternatively connected to the positive and negative terminals of a high voltage source (Figure 5 and 6). Such a PZT or PMN stack behaves like an electrical capacitor. When activated, the electroactive material expands and produces output displacement. Typical strains for electroactive materials are in the range 750-1200  $\mu\text{m}/\text{m}$ .

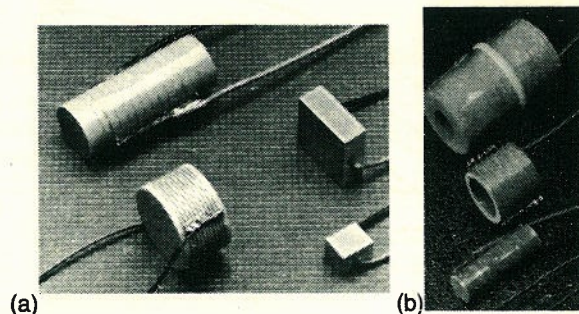


Figure 5 (a) small-size piezoelectric stacks. (b) Larger-size piezoelectric stacks (EDO Corporation).

PZT or PMN stacks are constructed by two methods. In the first method, the layers of active material and the electrodes are mechanically assembled and glued together using a structural adhesive. The adhesive modulus (typically, 4-5 GPa) is at least one order of magnitude lower than the modulus of the ceramic (typically, 70-90 GPa). This aspect may lead to a stack stiffness that is significantly lower than the stiffness of the basic ceramic material. In the second method, the ceramic layers and the electrodes are assembled in the "green" state, and then fired together (co-fired) and, possibly, subjected to a high isostatic pressure (HIP process) to increase density. This process ensures a much stiffer final product and, hence, a better actuator performance. However, the processing limitations, such as oven and press size, etc., limit the applicability of this process to small size stacks only.

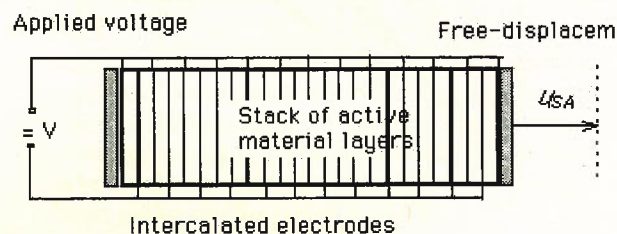


Figure 6 Induced strain actuator using a PZT or PMN electroactive stack

The PZT and PMN stacks are surrounded by a protective polymeric or elastomeric wrapping. Lead wires protrude from the wrapping for electrical connection. Steel washers, one at each end, are also provided for distributing the load into the brittle ceramic material. When mounted in the application structure, these stacks must be handled with specialized knowledge. Protection from accidental impact damage must be provided. Adequate structural support and alignment are needed. Mechanical connection to the application structure must be such that tension stresses are not induced in the stack since the active ceramic material has very low tension strength. Hence, the load applied to the stack must always be compressive and perfectly centered. If tension loading is also expected, adequate pre-stressing must be provided through springs or other means.

#### Construction of a TERFENOL Actuator

A magnetoactive solid-state actuator consists of a TERFENOL bar inside an electric coil and enclosed into an annular magnetic armature (Figure 7 and 8). When the coil is activated, the TERFENOL expands and produces output displacement. The TERFENOL material has been shown to be capable of strains up to 2000  $\mu\text{m}/\text{m}$ , but with highly nonlinear and hysteresis behavior. Practical strains employed by the



manufacturers of TERFENOL actuators are in the quasi-linear behavior range of 750-1000 mm/m.

The TERFENOL-D bar, the coil, and the magnetic armature, assembled between two steel-washers and put inside a protective wrapping, form the basic magnetoactive induced-strain actuator.

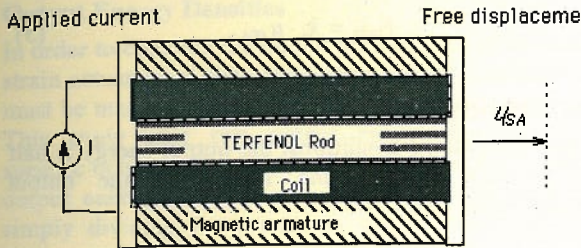


Figure 7 Induced strain actuator using a TERFENOL magnetoactive rod.



Figure 8 Magnetostrictive actuators with and without casing (ETREMA Products, Inc.).

#### Actuators with Casing and Pre-Stress Mechanism

Some commercially available solid-state actuators are just the drive units described above and shown in Figure 9. Other commercially available solid-state actuators also include a protective casing and a pre-stress mechanism. The casing provides protection for the active material and its electrical connections. It also facilitates the mechanical connection between the actuator and the application structure. The pre-stress mechanism is necessary to ensure that the active material is loaded in only compression, even when a moderate tension load is applied to its output rod. This issue is especially important with ceramic active materials (PZT and PMN) which are very weak in tension. When a pre-stress mechanism is incorporated, the protective casing also acts as a return path for the spring load, which usually makes the casing larger and heavier. The actuators with casing and pre-stress

mechanism can be directly fixed into the application structure, and do not require specialized knowledge from the user. However, the use of a spring has disadvantages from an energy output point of view, since some amount of energy will be stored in the spring and hence not delivered externally.

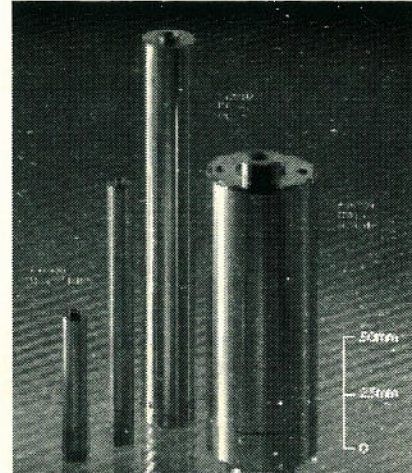


Figure 9 Piezoelectric actuators with casing (Politec PI, Inc.).

## THEORETICAL BACKGROUND

### Simplified Description of a Solid-State Actuator

In order to compare solid-state actuators of various material types and different operation principles, two overall performance parameters were selected:

- ISA displacement,  $u_{ISA}$ , measured in mm; and
- internal stiffness,  $k_i$ , measured in kN/mm or N/ $\mu$ m.

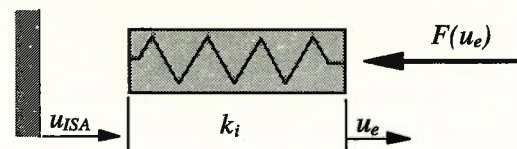


Figure 10 Induced strain actuator under external load  $F$

The ISA displacement,  $u_{ISA}$ , is the result of the induced-strain effect, which is the basic property of the active material.

Due to actuator compressibility, the external load,  $F(u_e)$ ,  $F(0)=0$ , produces an elastic displacement,  $F/k_i$ , where  $k_i$  is the internal stiffness (Figure 10). From the point of view of actuator effectiveness, the elastic compressibility displacement represents a loss. Since the internal stiffness of the actuator is finite, the application of an external load will always be accompanied by a compressibility loss. Hence, an



induced-strain actuator under load  $F$  will output only a fraction of its induced-strain displacement,  $u_{ISA}$ . Under load,  $F$ , the actuator output displacement,  $u_e$ , is given by:

$$u_e = u_{ISA} - \frac{F}{k_i} \quad (1)$$

When the external reaction load,  $F$ , is zero, the actuator output displacement,  $u_e$ , is maximum since no compressibility losses take place. The actuator displacement under zero external load is commonly known as "free stroke". Measurement of the actuator free stroke gives the value of the induced-strain actuator displacement,  $u_{ISA}$ . For nonzero external load, the actuator displacement,  $u_e$ , is always less than the induced-strain displacement,  $u_{ISA}$ . As the external load increases, the actuator displacement gets progressively smaller. Eventually, a point is reached where the external load is such that the compressibility loss balances the induced-strain displacement, and the resulting output displacement is zero. In other words, the actuator is "blocked". The actuator blocking load is given by

$$F_{blocking} = k_i \cdot u_{ISA} \quad (2)$$

Consider now that the external load,  $F$ , varies linearly with the output displacement,  $u_e$ , as for example in the presence of an external spring,  $k_e$ , as shown in Figure 9. Thus:

$$F = k_e \cdot u_e \quad (3)$$

Note that, in this case, the external load is entirely reactive, i.e., it takes place only in response to the actuator output displacement,  $u_e$ .

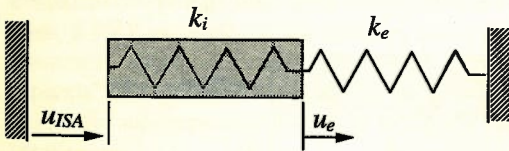


Figure 11 Induced strain actuator under external load  $F$

If the actuator output displacement is zero, then the external load is also zero. After substitution and simplification, one gets an expression for the output displacement,  $u_e$ , in terms of the stiffness ratio,  $r = k_e/k_i$ , i.e.,

$$u_e = \frac{1}{1+r} u_{ISA} \quad (4)$$

As the external stiffness,  $k_e$ , increases, the reaction force,  $F$ , also increases, and compressibility losses lead to diminishing output displacement. As the external stiffness tends to infinity, the whole induced-strain

displacement,  $u_{ISA}$ , is consumed internally, and the output displacement vanishes. This corresponds to the previously discussed "blocked" condition. Beyond this point, no further increase in the reaction force is possible. Thus, the maximum force of the actuator is realized when the actuator is blocked, i.e.,

$$F_{max} = k_i \cdot u_{ISA} \quad (5)$$

### Output Energy

Under quasi-static conditions, the output energy is half the product between the force and the output displacement, i.e.,

$$E_e = \frac{1}{2} k_e \cdot u_e^2 \quad (6)$$

Substitution of Equation (4) into Equation (6) yields the expression of output energy in terms of stiffness ratio,  $r$ , as:

$$E_e(r) = \frac{r}{(1+r)^2} \left( \frac{1}{2} k_i u_{ISA}^2 \right) \quad (7)$$

The variable part of Equation (7) is the output energy coefficient:

$$E'_e(r) = \frac{r}{(1+r)^2}$$

A plot of  $E'_e(r)$  as a function of  $r$  is given in Figure 12. The function  $E'_e(r)$  is zero for both "free" ( $r=0$ ) and "blocked" ( $r \rightarrow \infty$ ) conditions, and has a maximum at  $r=1$ . The  $r=1$  condition when  $k_e = k_i$ , is called "stiffness match". Thus, the maximum value of the output energy that can be delivered by an induced-strain actuator under the most favorable conditions is:

$$E'_{e\max} = \frac{1}{4} \left( \frac{1}{2} k_i u_{ISA}^2 \right)$$

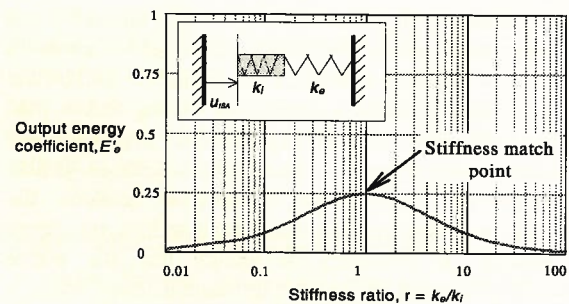


Figure 12 Stiffness match principle for peak energy delivery from an induced strain actuator

### Example

An actuator produces a free stroke  $u_{ISA} = 120 \mu\text{m}$ , and has an internal stiffness  $k_i = 370 \text{ kN/mm}$ . Under the



most favorable conditions (i.e., at stiffness match), the output energy will be:

$$E_{e\max} = \frac{1}{4} \left( \frac{1}{2} 370 \text{ kN/mm} \cdot (120 \mu\text{m})^2 \right) = 0.666 \text{ J}.$$

### Output Energy Densities

In order to compare the output performance of induced-strain actuators of different shapes and sizes, allowance must be made for their differences in volume and mass. This study uses two output energy densities: the specific output energy per unit volume and the specific output energy per unit mass. They are computed by simply dividing the maximum output energy by the volume and the mass of the actuator, respectively.

### Energy Conversion Efficiency

The output mechanical energy delivered at the output end of an induced-strain actuator is the result of electromagnetic energy applied at the input end of the induced-strain actuator. The conversion of electromagnetic energy into mechanical energy that takes place inside the actuator is a highly coupled process that will not be detailed here<sup>2</sup>. However, using simplified electric and magnetic energy expressions, one can derive first order approximations for the energy transformation efficiency that can serve as a basis for comparison between various actuators.

A first order approximation of the input electrical energy of solid-state induced-strain actuators based on electroactive materials (PZT and PMN), is given by:

$$E_{el} = \frac{1}{2} CV^2,$$

where C is the capacitance, and V is the voltage.

For solid-state induced-strain actuators based on magnetoactive materials (TERFENOL), a first approximation to the input electrical energy is given by:

$$E_{el} = \frac{1}{2} LI^2,$$

where L is the inductance and I is the current.

### DATA COLLECTION

A large variety of induced-strain actuators are presently available in the commercial market. In our study, we proposed to collect as much data as possible by directly

contacting the vendors and manufacturers of these products. A template of relevant input data was drafted. The template contained data entries for the induced-strain actuator and for the active material inside the actuator. Data entries regarding the induced-strain actuator were grouped under two headings: "General Data of the ISA Device" and "Data about the Active Material (PZT, PMN, TERFENOL, etc.)". These were detailed as follows:

#### "General Data of the ISA Device"

- Manufacturer (name, address, FAX/Phone, contact point):
- Device identification:
- Description (10 word max.):
- Maximum (free stroke) displacement, mm:
- Maximum force, N:
- Stiffness, kN/mm:
- Length, mm:
- Outside diameter, mm (or width  $\infty$  thickness, for rectangular cross-section, mm  $\infty$  mm):
- Mass, kg:
- Volume, cm<sup>3</sup>:
- Voltage, V, or current, A, as appropriate.:
- Capacitance,  $\mu\text{F}$ , or inductance, mH, as appropriate:
- Price, \$:

#### "Data about the Active Material (PZT, PMN, TERFENOL, etc.)"

- Active material diameter, mm (or width  $\infty$  thickness, for rectangular cross-section, mm  $\infty$  mm):
- Active material length, mm
- For stacked actuators, the layer thickness, mm, and the number of layers:
- Nonlinearity index, or a representative curve of the output displacement against electrical input:

Based on the above data, we set out to calculate and then to disseminate among the survey participants, the following comparative data:

- Apparent free strain, %:
- Apparent volume, cm<sup>3</sup>:
- Apparent density, 10<sup>3</sup>  $\infty$  kg/m<sup>3</sup>:
- Maximum deliverable energy per unit mass J/kg:
- Maximum deliverable energy per unit volume, J/cm<sup>3</sup>
- Maximum deliverable energy per unit cost, J/\$1000

The data template was sent to several prominent manufacturers of ISA materials and devices. The manufacturers contacted in our survey are listed below

<sup>2</sup> A detailed account of power delivery mechanism in an induced strain actuator is given by Giurgiutiu, and Rogers (1997).



in alphabetical order. Underlined are the manufacturers from which data has been received to date.

1. Burleigh Instruments, Inc., Burleigh Park, Fishers, NY 14453
2. EDO Corporation, 2645 South 300 West, Salt Lake City, Utah 84115
3. Etrema Products, Inc., 2500 North Loop Drive, Ames, Iowa 50010
4. Piezo Kinetics, Inc., P. O. Box 756, Pine St. & Mill Rd., Bellefonte, PA 16823
5. Piezo Systems, Inc., 186 Massachusetts Ave., Cambridge, MA 02139
6. TRS Ceramics Inc., Suite J, 2820 E. College Avenue, State College, PA 16801

Table 3 Basic data for selected induced strain actuators.

Identification	Type	Max. Free Expansion	Max. Force	Price	Active Material Outside Diameter	Active Material Inside Diameter	Active Material Area	Active Material Length	Stiffness	Active Material Volume	Active Material Mass
		$U_{ISA}$ ( $\mu$ m)	F (N)	(\$)	$D_o$ (mm)	$D_i$ (mm)	A ( $mm^2$ )	(mm)	$k_i$ (kN/mm)	$V_{ISA}$ ( $mm^3$ )	$m_{ISA}$ (g)
<b>Polytec PI</b>											
PZT (P-245.70)	HVPZT	120	2000	2010	10		78.5	101	32.0	7929	61.8
PZT (P-246.70)	HVPZT	120	12500	4975	25		490.6	100	200.0	49063	382.7
PZT (P-247.70)	HVPZT	120	30000	7900	35		961.6	100	400.0	96163	750.1
PZT (P-844.60)	LVPZT	90	3000	4665	9.9X10.9		100	109.9	65.0	10990	85.7
<b>EDO Corp.</b>											
PMN (E100P-4)	PMN	24	1500	275	11	0	95.0	26	150.0	2470	19.4
PMN (E300P-3)	PMN	42	9000	545	22	0	379.9	43	220.0	16337	128.2
PMN (E400P-1)	PMN	26	8600	265	25	10	412.1	27	330.0	11127	87.3
PMN (E400P-4)	PMN	60	8600	560	25	10	412.1	60	140.0	24728	194.1
<b>Kinetic Ceramics</b>											
D125160	HVPZT	160	28000	4530	31.75		791.3	144.78	153.2	114569	802.0
D125200	HVPZT	200	28000	5430	31.75		791.3	180.34	122.6	142708	999.0
<b>TOKIN</b>											
AE1010D16	LVPZT	18.4	3500	366	11.5x11.5	N/A	132.3	20	190.217	2000	21.2
ASB171C801	LVPZT	170	800	588	5x5	N/A	25	200	5.5	5000	40.0

Table 4 Basic data and mechanical performance of six induced strain actuators with casing and pre-stress mechanism

Identification	Type	Max. Free Expansion	Diameter	Length	Apparent Free Strain	Actuator Volume	Actuator Mass	Apparent Density	Maximum Output Energy	Output Energy per Actuator Volume	Output Energy per Actuator Mass
		$U_{ISA}$ ( $\mu$ m)	(mm)	(mm)	%	V ( $mm^3$ )	m (g)	kg/ $m^3$	$E_o$ (J)	$E_{ref}/V$ (J/ $dm^3$ )	$E_{ref}/m$ (J/kg)
<b>Polytec PI</b>											
P-245.70	HVPZT	120	18	125	0.096	31793	154	4844	0.05760	1.8117	0.3740
P-246.70	HVPZT	120	39.8	140	0.086	174086	830	4768	0.36000	2.0679	0.4337
P-247.70	HVPZT	120	50	142	0.085	278675	980	3517	0.72000	2.5837	0.7347
P-844.60	LVPZT	90	20	137	0.066	43018	215	4998	0.06581	1.5299	0.3061
<b>Kinetic Ceramics</b>											
D125160	HVPZT	160	38.1	185.42	0.086	211289	1450	6863	0.49034	2.3207	0.3382
D125200	HVPZT	200	38.1	218.44	0.092	248915	1163	4672	0.61290	2.4623	0.5270
<b>TOKIN</b>											
ASB171C801		170	19.6	213	0.080	64233	500	7784	0.01987	0.3093	0.0397



Table 5 Mechanical performance of selected induced strain actuators.

Identification	Apparent Density	Free Strain	Apparent Young's Modulus	Maximum Output Energy	Output Energy per Active Material Volume	Output Energy per Active Material Mass	Output Energy per Unit Cost	Cost per Unit of Energy
	$\rho_{ISA}$ (kg/m <sup>3</sup> )	%	E (GPa)	$E_o$ (J)	$E_o/V_{ISA}$ (J/dm <sup>3</sup> )	$E_o/m_{ISA}$ (J/kg)	$E_o/Price$ (mJ / \$1000)	Price/ $E_o$ (\$/mJ)
<b>Polytec PI</b>								
PZT (P-245.70)	7800	0.119	41.2	0.0576	7.265	0.931	28.7	\$ 34.90
PZT (P-246.70)	7800	0.120	40.8	0.3600	7.338	0.941	72.4	\$ 13.82
PZT (P-247.70)	7800	0.120	41.6	0.7200	7.487	0.960	91.1	\$ 10.97
PZT (P-844.60)	7800	0.082	71.4	0.0658	5.988	0.768	14.1	\$ 70.88
<b>EDO Corp.</b>								
PMN (E100P-4)	7850	0.092	41.1	0.0108	4.373	0.557	39.3	\$ 25.46
PMN (E300P-3)	7850	0.098	24.9	0.0485	2.969	0.378	89.0	\$ 11.23
PMN (E400P-1)	7850	0.096	21.6	0.0279	2.506	0.319	105.2	\$ 9.50
PMN (E400P-4)	7850	0.100	20.4	0.0630	2.548	0.325	112.5	\$ 8.89
<b>Kinetic Ceramics</b>								
D125160	7000	0.111	28.0	0.4903	4.280	0.611	108.2	\$ 9.24
D125200	7000	0.111	27.9	0.6129	4.295	0.614	112.9	\$ 8.86
<b>TOKIN</b>								
AE1010D16	10580	0.092	28.8	0.0081	4.025	0.380	22.0	\$ 45.47
ASB171C801	8000	0.085	44.0	0.0199	3.974	0.497	33.8	\$ 29.59

7. Polytec PI, Inc., 3001 Redhill Ave., Bldg. 5-102, Costa Mesa, CA 92626
8. Tokin America, Inc., 155 Nicholson Ln, San Jose, CA 95134
9. Kinetic Ceramics, Inc., 26242 Industrial Blvd., Hayward, CA 94545

The response of the manufacturers was extensive. Out of the large number of entries, we selected 12 representative actuators.

These include the actuators with the most outstanding performance from each vendor. For comparison, some actuators with lower performance were also included. Table 3 presents the basic data for the 12 selected actuators. Note that the length, diameter, volume and mass data in Table 3 only refers to the active material contained inside the actuator. For actuators without casing, these data is practically all that is required. For actuators with casing and pre-stress mechanism, more data is required.

The survey showed that many commercially available induced-strain products are delivered as basic units, without casing and pre-stress mechanism. We could identify three manufacturers that offer induced-strain products with casing and pre-stress mechanism. These manufacturers are Polytec PI, Tokin, and Kinetic Ceramics. The casing can be made of aluminum or steel.

The vendor Polytec PI produces a large variety of induced-strain actuators based on PZT electroactive material. Their products usually contain a pre-stressing spring. The piezoceramic actuators developed by Tokin and Kinetic Ceramics does not commonly include pre-stressing spring, and hence, care must be taken to ensure that only compressive load is applied. This precaution comes from the small strength in tension that is common to all ceramic materials. A number of seven actuators that can be delivered with casing and pre-stress mechanism were included in our study. For these actuators, the basic data must also include the overall length, diameter, volume and mass of the actuator. For the seven actuators included in our study, these data is given in Table 4. Note that the overall dimensions, volume and mass of the complete actuators are considerably larger than those for the active material alone. It is expected that this aspect will make the energy density of the actuator with casing and pre-stress mechanism sensibly lower than that of the active material alone.

## RESULTS

### Data Reduction

The collected data was processed to yield the following entries:



- Maximum output energy, defined as  $E_{e\max} = \frac{1}{4} \left( \frac{1}{2} k_i \cdot u_{ISA}^2 \right)$ , where  $k_i$  is the internal stiffness of the actuator and  $u_{ISA}$  is the maximum displacement (free stroke).
- Volume-based energy density, defined as reference energy per unit volume.
- Mass-based energy density defined as reference energy per unit mass.
- Cost-based energy density defined as reference energy per unit cost.
- Energy-based price defined as the cost of a unit of reference energy.
- Energy transformation efficiency.

The maximum output energy,  $E_{e\max} = \frac{1}{4} \left( \frac{1}{2} k_i \cdot u_{ISA}^2 \right)$ , was obtained directly from the data provided by the manufacturers. The energy densities per unit volume and unit mass were obtained by dividing by the relevant volume and mass.

Table 6 Comparison of mechanical and electrical performance of selected induced strain actuators

Identification	Output Mechanical Energy	Voltage	Electric Capacitance	Number of Layers	Layer Thick.	Electrical Input Energy	Energy transformation efficiency
	$E_e$ (J)	(V)	( $\mu$ F or mF)		(mm)	(J)	(%)
<b>Polytec PI</b>							
PZT (P-245.70)	0.05760	1000	0.5	183	0.500	0.2500	23.0%
PZT (P-246.70)	0.36000	1000	3.28	178	0.500	1.6400	22.0%
PZT (P-247.70)	0.72000	1000	6.56	178	0.500	3.2800	22.0%
PZT (P-844.60)	0.06581	100	43.00	999	0.110	0.2150	30.6%
<b>EDO Corp.</b>							
PMN (E100P-4)	0.01080	800	0.09	14	0.500	0.0288	37.5%
PMN (E300P-3)	0.04851	800	1.10	46	0.500	0.3520	13.8%
PMN (E400P-1)	0.02789	800	0.50	28	0.500	0.1600	17.4%
PMN (E400P-4)	0.06300	800	1.25	28	0.500	0.4000	15.8%
<b>Kinetic Ceramics</b>							
D125160	0.49034	1000	8.20	178	0.500	4.1000	12.0%
D125200	0.61290	1000	10.50	178	0.500	5.2500	11.7%
<b>TOKIN</b>							
AE1010D16	0.00805	150	5.4	N/A	N/A	0.0608	13.3%
ASB171C801	0.01987	150	15	N/A	N/A	0.1688	11.8%

### Results Based on Active Material Volume and Mass

Table 5 presents the mechanical performance of all the 12 selected induced strain actuators based on active material volume and mass. The maximum output energy and the output energy densities based on active material volume and mass are given. Also given in Table 5 are the output energy per unit cost, and it inverse, the cost of a unit of output energy.

### Results Based on Actuator Volume and Mass

Table 4 presents, in its last two columns, the mechanical performance energy indicators based on volume and mass. By comparing the entries in Table 4

and in Table 5 for the same actuator, it can be seen that the addition of casing and pre-stress mechanism significantly lowers the energy density of the device.

Table 7 Ranking of 12 induced-strain actuators in terms of maximum output energy, energy densities with respect to active-material volume and mass, cost, and with respect to actuator volume and mass for the actuators with a casing and pre-stress mechanism.

Identification	Maximum Output Energy	Output Energy per Active Material Volume	Output Energy per Active Material Mass	Output Energy per Unit Cost	Output Energy per Actuator Total Volume	Output Energy per Actuator Total Mass
<b>Polytec PI</b>						
PZT (P-245.70)	7	3	3	10	5	5
PZT (P-246.70)	4	2	2	7	4	2
PZT (P-247.70)	1	1	1	5	1	1
PZT (P-844.60)	5	4	4	12	6	6
<b>EDO Corp.</b>						
PMN (E100P-4)	11	5	7	8		
PMN (E300P-3)	8	10	10	6		
PMN (E400P-1)	9	12	12	4		
PMN (E400P-4)	6	11	11	2		
<b>Kinetic Ceramics</b>						
D125160	3	7	6	3	3	4
D125200	2	6	5	1	2	3
<b>TOKIN</b>						
AE1010D16	12	8	9	11		
ASB171C801	10	9	8	9	7	7

### Results Based on Energy Conversion Efficiency

A comparison of the mechanical and electrical performance of the actuators is given in Table 5. The maximum output mechanical energy, and the electrical energy necessary to produced this output are given. Division of the output mechanical energy by the input electrical energy yields the energy conversion efficiency of the induced-strain actuator. The energy conversion efficiency is given in the last column of Table 6.

### Ranking of the Induced-Strain Actuators

Table 7 presents the ranking of the 12 induced-strain actuators considered in the study. The ranking is done in decreasing order. The actuators with the best performance are ranked first, while those with the less desirable performance are ranked last. Examination of Table 7 indicates that some rank variations exist that can be related to the type of criteria used. However, a clear distinction can be drawn between actuators with high performance, and actuator with low performance. It is interesting to note that actuators of widely different performance ranking exist within the product line of the same manufacturer, as for example under the entries for Polytec PI. The ranking is just a first-order comparison of the considered actuators, since every specific application will have its own requirements.



### Consistency Checks

To impart increased credibility to the numerical results, and to filter out any inadvertent discrepancies, a number of consistency checks were performed. First, it was noticed that our study computed the energy density of active material by simply dividing the maximum output energy by the active material volume and mass provided by the manufacturer. However, the energy density could also be correlated with other basic material data, such as:

- free strain,  $e_{ISA}$ , defined as the ratio between the free displacement,  $u_{ISA}$ , and the length,  $L$ .
- apparent Young's modulus,  $E$ , defined from the stiffness formula  $k_i = EA/L$ , where  $A$  is the cross-sectional area of the stack.

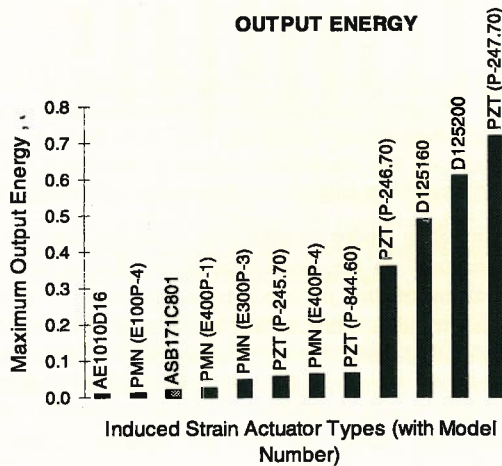


Figure 13 Comparison of output energy for commercially available induced strain actuators including piezoelectric (PZT), electrostrictive (PMN)

The free strain was calculated by dividing the free displacement by the active material length. The apparent Young's modulus was calculated from the formula  $k_i = EA/L$  when the active material stiffness was available. This is especially the case with glued stacks, where the compliance of the adhesive layer lowers significantly the stiffness of the stack. In certain situations, the active material stiffness was not available. Then, general values of the material Young's modulus as available from the manufacturer were used to calculate the active material stiffness. For example, for the Morgan Matroc products, we used  $E_{PZT-5} = 48$  GPa.

It should be noted that the volume-based energy density can also be calculated by the well-known formula

$E_{e_{max}} / V = \frac{1}{4} \left( \frac{1}{2} E e_{ISA}^2 \right)$ . A further division by the equivalent material density,  $\rho$ , yields the mass-based energy density,  $E_{e_{max}} / m = \frac{1}{\rho} \frac{1}{4} \left( \frac{1}{2} E e_{ISA}^2 \right)$ . Based on these observations we performed consistency checks on our results.

### DISCUSSION OF RESULTS

The results presented in Tables 3 through 6 were used to construct comparative charts presented in Figures 13 through 19

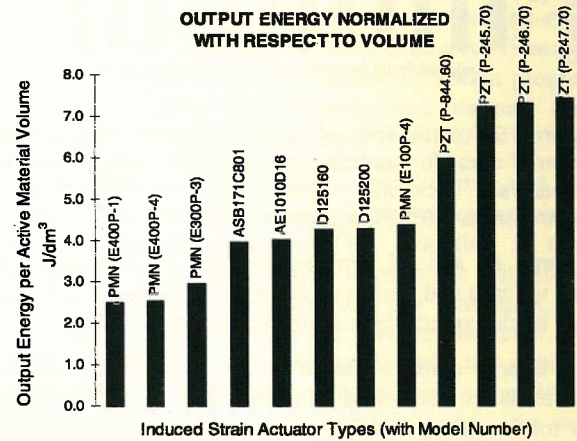


Figure 14 Comparison of output energy per active material volume for commercially available induced strain actuators including piezoelectric (PZT) and electrostrictive (PMN) active materials

These charts give a quick visual perception of the relative performance of the actuators in terms of maximum output energy, output energy densities, and energy conversion efficiency.

Figure 13 presents a comparison of the maximum output energy that can be extracted from the commercially-available induced-strain actuators currently on the market. It seems that, at present, only two companies, Polytec PI, Inc. and Kinetic Ceramics, have products with large energy capability (P-247-70, D125200, D125160 and P246-70). When this aspect was discussed with the other vendors, it was argued that they can also manufacture products with similar output energy, but on special order.

Figure 12 compares the energy density per unit volume. For high-performance induced-strain actuators, a mid-range value of around 6-7.5 J/dm³ seems to be common.

Figure 15 compares the energy density per unit mass of active material. For high-performance induced-strain



actuators, a mid-range value of around 0.7-0.9 J/kg seems to be common.

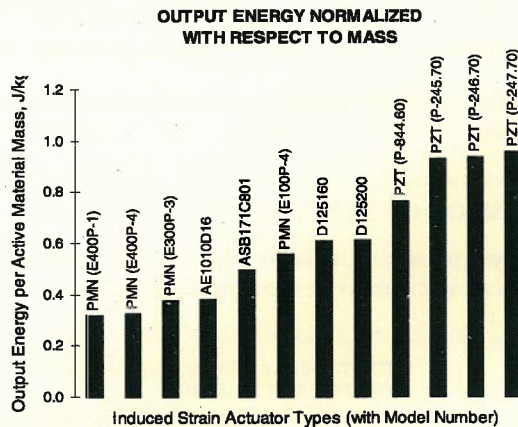


Figure 15 Comparison of output energy per active material mass for commercially available induced strain actuators including piezoelectric (PZT) and electrostrictive (PMN) active materials

Figures 16 and 17 compare the energy densities per unit volume and unit mass for the six actuators that can also be delivered with casing and pre-stress mechanism.

The energy densities based on active material volume and mass are contrasted with the energy densities based on total actuator volume and mass. It can be noticed that the addition of casing and pre-stress mechanism greatly reduces the energy density of the device. This reduction is more pronounced in terms of energy density per unit volume than in terms of energy density per unit mass.

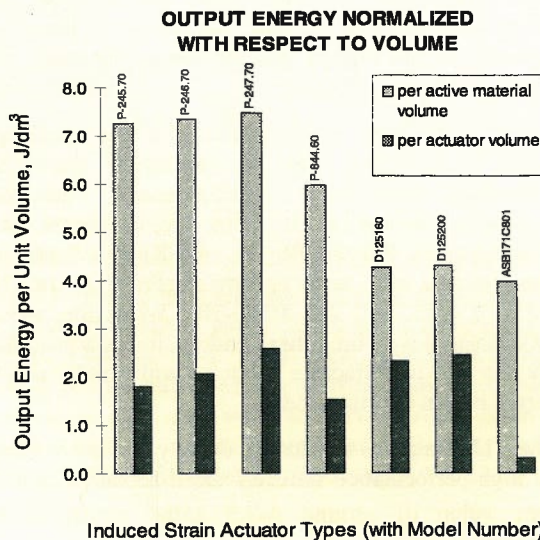


Figure 16 Comparison of output energy density per unit volume for 6 induced-strain actuators with casing and pre-stress mechanism, showing that the addition of

casing greatly reduces the volume-based energy density due to the large relative volume of the casing.

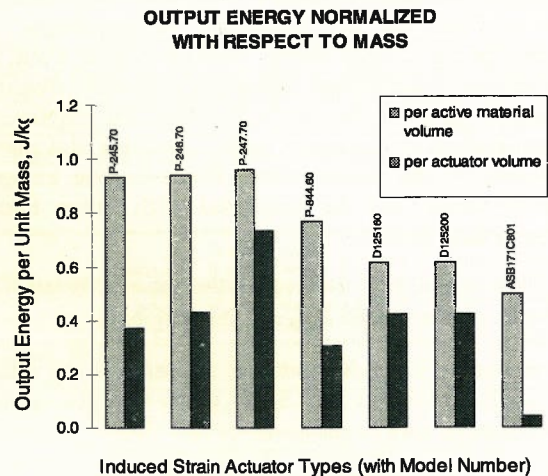


Figure 17 Comparison of output energy density per unit mass for 7 induced-strain actuators with casing and pre-stress mechanism, showing that the addition of casing reduces the mass-based energy density due to inactive mass of the casing and pre-stress mechanism.

For applications where volume and mass are essential, as for example in the aerospace industry, the direct incorporation of the induced-strain actuator without casing and pre-stress mechanism in the host structure is highly desirable since it leads to important volume and mass savings. Figures 18 compares energy density based on unit cost in mJ/\$1000.

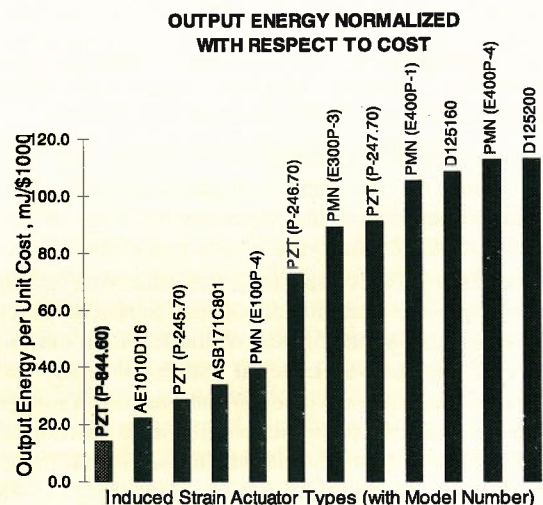


Figure 18 Comparison of output energy per unit cost for commercially available induced strain actuators including piezoelectric (PZT), electrostrictive (PMN) active materials.



Examination of this chart indicates that some companies are capable of marketing products with remarkably lower specific energy cost than others. This observation does not seem to be influenced by the processing method, since it equally affects adhesively-bonded and co-fired actuator products.

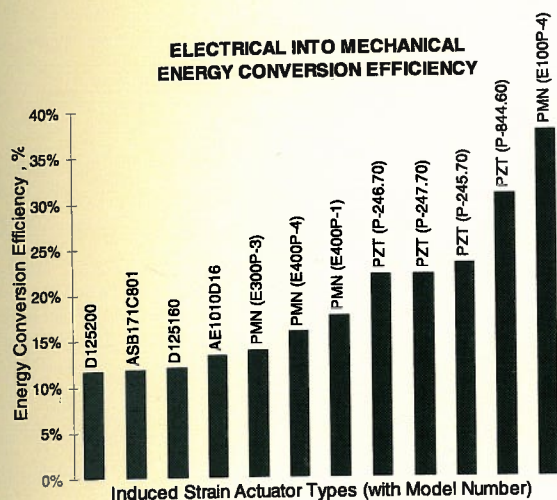


Figure 19 Comparison of electrical into mechanical energy conversion efficiency for commercially available induced strain actuators including piezoelectric (PZT), electrostrictive (PMN) active materials.

Finally, Figure 19 presents a comparison of the energy conversion efficiency from input electrical energy into output mechanical energy. It should be mentioned that the formulae used to estimate the required input electrical energy are only first order approximations since they ignored the variation or capacitance and inductance in the presence of an applied external load. Also, the energy dissipation in internal electric resistance and in hysteresis is, for the moment, ignored. Figure 19 shows that, for high-performance induced-strain actuators based on electroactive materials the energy transformation efficiency is around 20%. This does not mean that the remaining 80% of energy is lost, but that it simply does not get converted into mechanical energy and is sent back to the power source.

## CONCLUSIONS

An energy-based comparison of commercially-available induced-strain actuators (ISA) was presented. The data was collected from a survey of prominent manufacturers of ISA materials and devices, who responded with enthusiasm to our request for information.

The comparison, presented in the accompanying tables and charts, shows that output energy values of up to

0.72 J can be achieved with off-the-shelf commercially-available actuators. Energy density per unit volume of active material was found in the range 2.5-7.5 J/dm<sup>3</sup>. Energy density per unit mass of active material was found in the range 0.31-0.96 J/kg. Energy transformation efficiency between input electric energy and output mechanical energy was found to be: 11.7-37.5% for adhesively-bonded PZT and PMN stacks. The overall performance of induced-strain actuators, when compared on the basis of output energy density, was found to vary widely from vendor to vendor, and even from one model to another within the same vendor catalogue list. The variations from vendor to vendor may be attributed to architectural differences in the detailed mechanical construction of the induced-strain actuators. The variations between products offered by the same vendor may be explained by recent progress in the active material technology that has only been incorporated in the latest products.

It was observed that the addition of casing and pre-stress mechanism greatly reduces the energy density of an induced-strain actuator. This reduction is more pronounced in terms of energy density per unit volume than in terms of energy density per unit mass. For applications where volume and mass are essential, it is highly desirable to incorporate directly the induced-strain actuator in the host structure and to avoid the unnecessary addition of casing and pre-stress mechanism by proper design architecture of the local structure.

This study presented here went beyond simply comparing the properties of various active materials exhibiting the induce-strain actuating effect. In this study, assembled induce-strain actuators, directly available on the commercial market, were considered and compared. The advantage of our approach is that it offers data that can be directly incorporated in the design of mechanical and hydraulic devices utilizing off-the-shelf induced-strain actuators.

## ACKNOWLEDGMENTS

The authors gratefully acknowledge the support of the Army Research Office – Proposal 41214-EG, Dr. Gary Anderson, Program Manager.

The authors would also like to thank all the contact persons in the companies participating in this survey. Their extended help, guidance and constructive intellectual interaction were extremely useful in clarifying some of the more subtle points encountered during the survey.



## REFERENCES

1. Furuya, Y., Watanabe T., Hagood N.W., Kimura H., Tani J., "Giant Magnetostriction of Ferromagnetic Shape Memory Fe-Pd Alloy Produced by Electromagnetic Nozzleless Melt-Spinning Method", 9<sup>th</sup> International Conference on Adaptive Structures and Technologies, Boston, MA, October 14-16, 1998.
2. Galvagni, J., Rawal, B., "A Comparison of Piezoelectric and Electrostrictive Actuator Stacks", Paper 1543-50, SPIE Vol. 1543 Adaptive and Adaptive Optical Components", 1991, pp. 296-300.
3. Giurgiutiu, V., Chaudhry, Z., Rogers, C.A., "Effective Use of Induced-strain Actuators in Aeroelastic Vibration Control", Proceedings of the Adaptive Structures Forum, 35th AIAA/ASME/ASCE/AHS/ASC Structures, Structural Dynamics, and Materials Conference, New Orleans, LA, April 13-14, 1995, Paper # AIAA-95-1095.
4. Giurgiutiu, V., Chaudhry, Z., Rogers, C.A., 1995b, "Stiffness issues in the Design of ISA Displacement Amplification Devices: Case Study of a Hydraulic Displacement Amplifier", Smart Structures and Materials '95, San Diego, CA, 26 February -3 March 1995, Paper # 2443-12
5. Giurgiutiu, V., Chaudhry, Z., Rogers, C.A., 1994, "The Analysis of Power Delivery Capability of Induced-strain Actuators for Dynamic Applications", Proceedings of the Second International Conference on Intelligent Materials, ICIM'94, June 5-8, 1994, Colonial Williamsburg, VA, Technomic Pub. Co., Inc., 1994, pp. 565-576.
6. Giurgiutiu, V., and Rogers C. A., "Power energy characteristics of Solid State Induced-Strain Actuators for Static and Dynamic Applications", Journal of Intelligent Material Systems and Structure, Vol. 7, pp. 656-667, 1996.
7. Janker, P., Martin, W., "Performance and Characteristics of Actuator Material", 4th International Conference on Adaptive Structures, Koln, Germany, pp. 126-138, 1993.
8. Lee T. and Chopra I, "Design and Testing of a Trailing-Edge Flap Actuator with Piezostacks for a Rotor Blade", SPIE Conference on Smart Structures and Integrated Systems, San Diego, CA, 1998.
9. Park, S.-E., and Shrout T. R., "Ultrahigh strain and piezoelectric behavior in relaxor ferroelectric single crystals", Journal of Applied Physics, Vol. 4, No. 82, pp. 1804-1811, 1997
10. Straub, F. K., and Merkley, D. J., "Design of a Smart Material Actuator for Rotor Control", 1995 SPIE North American Conference on Smart Structures and

Materials, Smart Structures and Integrated Systems, San Diego, CA, 26 February - 3 March 1995, Paper # 2443-10.